

Investigation of Polymer Hybrid Ball Bearings' Dynamic Behaviour

Burcu KÜÇÜKOĞLU DOĞAN^{1*}, Tuncay KARAÇAY²

¹Muş Alparslan University, Faculty of Engineering and Architecture, Department of Mechanical Engineering, Muş/Turkey.
ORCID: 0000-0002-0447-9456

²Gazi University, Faculty of Engineering and Architecture, Department of Mechanical Engineering, Ankara/Turkey.
ORCID: 0000-0002-6014-5610

Corresponding Author: b.kucukoglu@alparslan.edu.tr

Arrival Date: 28.11.2023

Acceptance Date: 19.12.2023

Abstract

Contact mechanics must be analyzed to determine the dynamic characteristics of polymer hybrid bearings. Since the polymer bearings have contact surfaces of polymer-polymer, polymer-glass, or polymer-steel, the Hertz contact theory used to examine the contact mechanics of conventional bearings cannot be directly used. Due to the elastoplastic structure of polymer materials, elastoplastic contact mechanics is used in examining contact mechanics. In this study, the contact mechanics of the polymer bearing were analyzed as elastoplastic contact and were included in the shaft-bearing system model. An algorithm was developed in the MATLAB environment using the geometry of the 6203 bearings, and its dynamic characteristics were examined through simulations. The equations of motion are simulated at different shaft speeds with an elastic region assumption to determine the dynamic characteristics of polymer hybrid bearings. The results are discussed in the time-frequency domain.

Keywords: Elasto-Plastic Contact, Polymer Hybrid Ball Bearing, Vibration

Polimer Hibrid Rulmanların Dinamik Davranışının İncelenmesi

Özet

Polimer hibrid rulmanların dinamik özelliklerini belirlemek için temas mekaniğinin analiz edilmesi gerekmektedir. Polimer rulmanlar polimer-polimer, polimer-cam veya polimer-çelik temas yüzeylerine sahip olduğundan, geleneksel rulmanların temas mekaniğini incelemek için kullanılan Hertz temas teorisi doğrudan kullanılamamaktadır. Polimer malzemelerin elastoplastik yapısından dolayı temas mekaniğinin incelenmesinde elastoplastik temas mekaniği kullanılmaktadır. Bu çalışmada, polimer hibrid rulmanın temas mekaniği elastoplastik temas olarak analiz edilmiş ve shaft-rulman sistemi modeline dahil edilmiştir. 6203 rulmanın geometrisi kullanılarak MATLAB ortamında bir algoritma geliştirilmiş ve simülasyonlar aracılığıyla dinamik özellikleri incelenmiştir. Polimer hibrid rulmanların dinamik özelliklerini belirlemek için hareket denklemleri rulmanın elastik bölgede olduğu kabul edilerek farklı mil hızlarında simüle edilmiştir. Sonuçlar zaman-frekans alanında tartışılmıştır.

Anahtar Kelimeler: Elasto-Plastik Temas, Polimer Hibrid Rulman, Titreşim

1. INTRODUCTION

Polymer bearings, unlike steel bearings, have recently become more common in industry because they provide more advantages in places where the load-carrying capacity is not essential, hygiene is required, chemicals are used, and a quiet working environment is required. Polymer hybrid bearings are generally made of polymer inner race, outer race, and cage, and rolling elements (balls) could be polymer, glass, or steel balls, depending on the application. Figure 1 shows the unassembled view of the polymer hybrid deep groove ball bearing used in the simulations.



Figure 1. The distributed view of polymer hybrid deep groove ball bearing

The long lifespan of bearings is essential in terms of economy and continuity of production. For this reason, bearings are operated within the limits of the elastic region. Hertz contact is used to analyze the contact mechanics of conventional steel bearings. However, the polymer ball bearings' structure differs from steel bearings because the balls and races consist of different materials. So, Hertz's contact theory cannot be directly used to examine the contact in polymer bearings. When examining the contact mechanics of polymer bearings, elastoplastic contact is used instead of Hertz contact theory. Elasto-plastic contact examines elastic, elasto-plastic, and fully plastic regions in three parts and two kinds of model: the indentation model and the flattening model. The critical deformation rate must be known to classify the contact area formed in elasto-plastic contact, which is explained in detail in Section 2.

In elasto-plastic contact, the critical deformation rate, first proposed by Kogut and Etsion and later by Jackson and Green, to which the von Mises yield criterion of the material was added, is used to determine in which region the contact occurs. Kogut and Etsion determined frictionless elasto-plastic contact between the deformable sphere and the rigid surface. They indicated when contact $\delta/\delta_c \leq 1$ there is a fully elastic region, and it is compatible with Hertzian contact when $1 < \delta/\delta_c \leq 6$ a plastic zone has started under the sphere surface, but the whole contact area is elastic; when $6 < \delta/\delta_c \leq 68$ there is elastic-plastic contact, and when $\delta/\delta_c > 68$ the contact area is in the fully plastic region [2]. Later, unlike the model created by Kogut and Etsion, Jackson and Green added geometry and material effects to the model and created a model using the finite element method, accepting the Von Mises yield strength criterion as the yield point of the material and accepting it as $\delta/\delta_c < 1.9$ the elastic region. This model can use the material's yield point with the two deformable surfaces' weaker and lower yield points [3, 4]. Brake developed a new formulation for the elasto-plastic contact of two circular objects in the normal direction, taking into account the contact geometry and material properties [5]. Jamari and Schipper created a theoretical model for the elasto-plastic contact of ellipsoid bodies [6]. Zhao et al. modeled three regions between two flat surfaces: elastic, elasto-plastic, and plastic regions, and used the hardness of the material to determine the critical contact point [7]. Li et al. examined the rigid and elastoplastic spheres by modifying the theoretical model created by Johnson [8]. Jackson and Sharma investigated the cylindrical elasto-plastic contact between a solid flat surface and a cylinder modeled as a deformable quarter circle using the finite element method [9]. Yau et al. used elasto-plastic models to determine the stress distribution on the bearing in the elastic and elasto-plastic regions [10,11]. Komvopoulos and Song examined the deformation of elasto-plastic half-space and rigid cylindrical contact in four different deformation forms: linear elastic-plastic, nonlinear elastic-plastic, transition to full plastic and the steady-state part of plastic deformation using the finite element method [12].

Elasto-plastic contact is examined with two models: the indentation model and the flattening model. Some researchers have examined various contact surfaces using only the indentation and flattening contact model. Ghaednia et al. investigated the frictionless contact between an elasto-plastic surface and a sphere. They achieved this by developing a novel model that connects the flattening and indentation models, allowing for elasto-plastic deformation of both surfaces. [1]. Ogar et al. analyzed the flattening model with a sphere, considering the material's hardness with the finite element method [13]. Deng et al. investigated the similarities and differences between the elasto-plastic flattening and indentation contact model with the finite element method using five different materials whose yield strengths cover a typical range of steel materials used in engineering [14]. Ogar et al. investigated indentation and flattening in the contact between a rigid, rough surface and an elasto-plastic half-space, as well as between a rigid, smooth surface and a rough surface [15]. Jackson and Kogut examined the indentation and flattening contact model comparatively using the finite element method [16]. Mesarovic and Fleck examined the indentation contact between a rigid sphere and an elasto-plastic deformable surface with and without considering friction [17]. Sara et al. used slip-line theory to investigate the yield force and average pressure of the indentation

contact between the rigid sphere and the frictionless deformable surface, and they compared their findings with those obtained using the finite element method. [18].

Bearings have complex dynamics, unlike their simple structures. Bearings produce vibration even when they are healthy. When the vibration of healthy bearings is examined, high amplitude signals are seen at the frequency values known as Ball Pass Frequency. Gustafsson and Tallian first determined the Ball Pass Frequency (BPF) with a mathematical model [19,20]. Meyer et al. decided that Ball Pass Frequency (BPF) and its harmonics are seen even if the bearing is healthy after Gustafsson and Tallian's study [21,20].

This study models the shaft-bearing system mathematically to predict how bearings behave dynamically. The contact mechanics between the ball and races are also investigated and introduced to the shaft-bearing model. The dynamic behaviors of healthy and faulty bearings were compared with simulations at different shaft speeds and under various loading conditions [22,23,24,25]. The mathematical model of the 6203 series deep groove ball bearing with steel balls has two degrees of freedom along lateral and vertical, and simulations are run under elastic contact assumption.

2. ELASTO-PLASTIC CONTACT MODEL

a) Indentation Model

The indentation model was modeled to determine the contact between the sphere and the flat surface. According to this model, the hardness of the contacting surfaces is different from each other. Of the contacting surfaces, the sphere is more rigid, and the material used for the flat surface is softer than the material used for the sphere. Since the surface is more delicate, it is accepted that deformation occurs on the contact surface [1]. Figure 2 shows the schematic view of the indentation model.

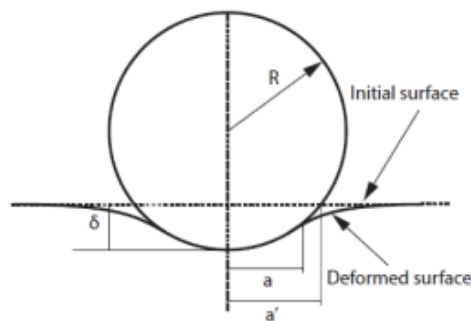


Figure 2. Indentation model [1]

b) Flattening Model

The flattening model is the other model of the elastoplastic model. In contrast to the indentation model, it is modeled to establish the contact model of the soft sphere, and the more rigid flat surface sphere is constructed of softer material in this model. Deformation is assumed to occur on the sphere using the contact model. Figure 3 shows the schematic view of the flattening model.

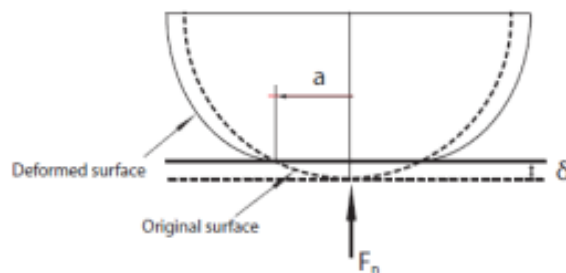


Figure 3. Flattening model [1]

To determine the contact area in elasto-plastic contact, the deformation ratio to the critical deformation amount is mathematically calculated using the contact properties of the contacting surfaces.

Critic Deformation

Critical deformation is an important criterion used to determine where the contact area occurs and is calculated by considering the material properties and geometries of the contacting surfaces. The mathematical formulation for the critical deformation amount is given in Eq. 1 [1,4].

$$\delta_c = \left(\frac{\pi \cdot C \cdot S_y}{2E'} \right)^2 R \quad (1)$$

$$\frac{1}{E'} = \frac{1-\nu_1^2}{E_1} + \frac{1-\nu_2^2}{E_2} \quad (2)$$

$$C = 1.295e^{0.736\nu_1} \quad (3)$$

E' indicates the equivalent elasticity modulus and is calculated using the formulation in Eq. 2 [1,4]. The elasticity modulus values of the materials from which the contacting objects are used in Eq. 1 are manufactured and calculated using the formulation given in Eq. 2. C is a constant specified by the mathematical formula shown in Eq. 3 [1,4]. R represents the radius of the sphere. This study calculates R by taking the resultant of the ball radius and the distances between the inner and outer race curvature radii. S_y is the yield stress value of the first deformed material. The coefficient vs seen in Eq. 3, used when calculating the constant C , represents the Poisson ratio of the first deformed material.

3. CONTACT MECHANICS

3.1. Total Deflection of Ball Bearing

Bearings transmit forces by deflection on the ball. The amount of deflection resulting from ball-inner race contact and ball-outer race contact is expressed as total deflection. The total deflection formulation is given in Eq. 4 [27]. δ_i indicates inner race-ball deflection, appears δ_2 in Figure 4, and δ_o indicates outer race-ball deflection δ_1 appears in Figure 4, δ the sum of the deformations on the ball as seen in Figure 4.

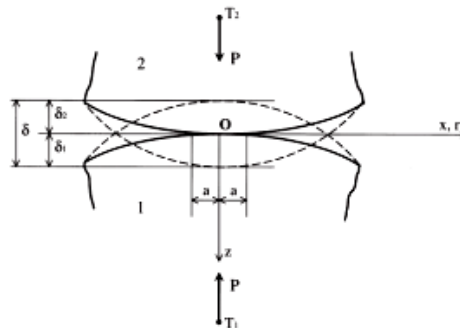


Figure 4. Total deflection of bearing [26]

$$\delta = \delta_i + \delta_o \quad (4)$$

$$\delta = \delta^* \left(\frac{3}{2} \frac{F}{\Sigma \rho} \left[\frac{1-\nu_1^2}{E_1} + \frac{1-\nu_2^2}{E_2} \right] \right)^{\frac{2}{3}} \frac{\Sigma \rho}{2} \quad (5)$$

The total deformation occurring on the bearing depends on the properties of the material used in the production of the parts forming the bearing and the geometric properties of the bearing. Eq. 5 indicates the mathematical representation of the amount of deformation calculated using the bearing's geometric properties and material properties [27]. The contact between the ball and the races has a point contact due to the structure of the balls and races. However, the point contact between the ball and the race turns into an elliptical area after loading. Primary and secondary elliptic integrals compute the parameters (a^* , b^* , and \square^*) needed to determine the contact area and deformation amount since the produced contact is elliptical. The dimensions of the elliptical area occurring in Hertz elastic contact and the deformation quantity can be roughly approximated when a^* , b^* , \square^* and dimensionless parameters are calculated.

3.2. Shaft-bearing system of polymer bearing

The shaft bearing system produces vibration even when the bearing on the system is healthy [21, 4]. This vibration is equal to the product of the cage frequency and the number of balls in the bearing and is called the Ball Pass Frequency (BPF). The equation used to determine the Ball Pass Frequency is given in Eq. 6. For this formulation, m represents the number of balls, and ω_c represents the angular velocity of the cage. The mathematical formulation seen in Eq. 7 calculates the angular velocity of the cage, and γ seen in Eq. 7 indicates the angle between the ball-bearing balls. Since the bearing used in this study is a deep groove ball bearing, α is taken as zero, as seen in Eq. 8.

$$\omega_{bg} = m\omega_c \quad (6)$$

$$\omega_c = \frac{1}{2}(\omega_i(1-\gamma) + \omega_o(1+\gamma)) \quad (7)$$

$$\gamma = \frac{d_b}{d_m} \cos \alpha \quad (8)$$

The force on the bearing is calculated by the total deflection and stiffness, as seen in Eq. 9. F indicates the total force on the bearing, K denotes the bearing stiffness, and δ indicates the total deformation amount on the balls.

$$F = K\delta^{3/2} \quad (9)$$

There is a nonlinear relationship between deflection and load, as seen in Eq. 9. To determine the nonlinear shaft-bearing system's dynamic behavior, the system's time solution at different loads and speeds must be obtained. For the theoretical part of this study, some assumptions were made, and the equations of motion were obtained.

The assumptions made are stated below;

- The shaft is assumed to have two degrees of freedom, x , and y , in the radial direction.
- The balls are placed at equal intervals around the inner and outer races. The outer race does not rotate.
- Balls are assumed to be massless.
- Races are rigid, and only local deformations occur.
- The shaft is assumed to be rigid.

The schematic view of the shaft-bearing system is given in Figure 5;

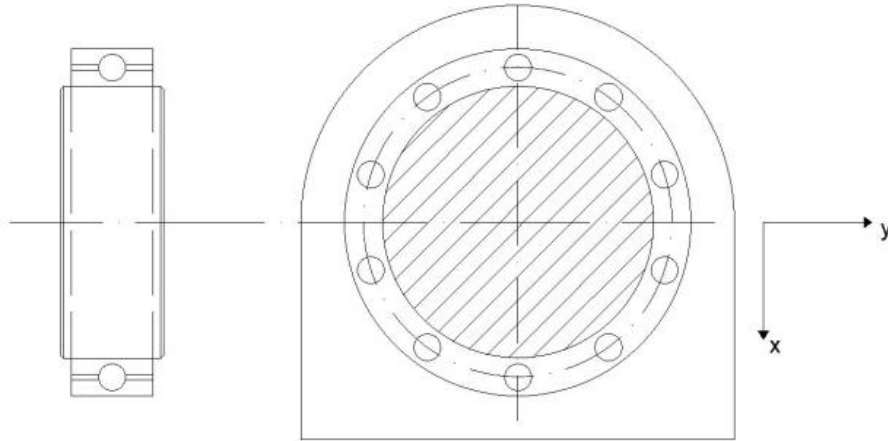


Figure 5. The schematic view of the shaft-bearing system

According to these assumptions, the equations of motion of the system model with two degrees of freedom are Eq. 11 and Eq. 12, which are stated below;

$$M\ddot{x} + \sum_{i=1}^n K_i \delta_i^{3/2} \cos(\theta_i) + P_x - Mg = 0 \quad (11)$$

$$M\ddot{y} + \sum_{i=1}^n K_i \delta_i^{3/2} \sin(\theta_i) + P_y = 0 \quad (12)$$

The equations of motion were solved using the fourth-order Runge-Kutta method and iterative methods. The system was solved with only the initial conditions to determine the system's natural frequency. P_x is the force in the x-axis direction and indicates the force on the bearing calculated by considering gravity's effect. P_y indicates the force acting on the bearing in the y-axis direction.

4. RESULTS AND DISCUSSION

The geometry of the bearings, the quantity of rolling elements, rotational speeds, and system operating factors all affect how dynamically a bearing behaves. The bearings' geometric and material characteristics were included in a mathematical model. MATLAB is used to develop a code that simulates the mathematical model with differential equation solutions. The code is run for different shaft speeds, and vibration spectra are obtained for these speeds. In order to analyze dynamic characteristics in the time-frequency domain, waterfall diagrams are plotted for the simulated 6203 series polymer hybrid ball bearing in good and faulty condition. The 6203 deep groove ball bearing properties used for simulations are given in Table 1, and the x-axis direction waterfall graph and y-axis waterfall graph are shown in Figure 6 and Figure 7, respectively.

Table 1. Properties of 6203 ball bearing

The diameter of the inner race	D_i	0,017 m
The diameter of the inner raceway	d_i	0,02358 m
Outer raceway diameter	d_o	0,02841 m
Outer race diameter	D_o	0,04 m
Bearing width	w	0,012 m

Balls Diameter	d_b	0,00426 m
Radius of inner race groove	r_i	0,002480 m
Outer race groove radius	r_o	0,003340 m
Number of balls	m	10
Contact angle	α	0

In Figure 6, the resonance of the shaft-bearing system is clearly visible when the Ball Pass Frequency coincides with the shaft's natural frequency (critical speed) along the x-axis at 3050 rpm. The natural frequency of the shaft along the x-axis is determined as 212,40 Hz.

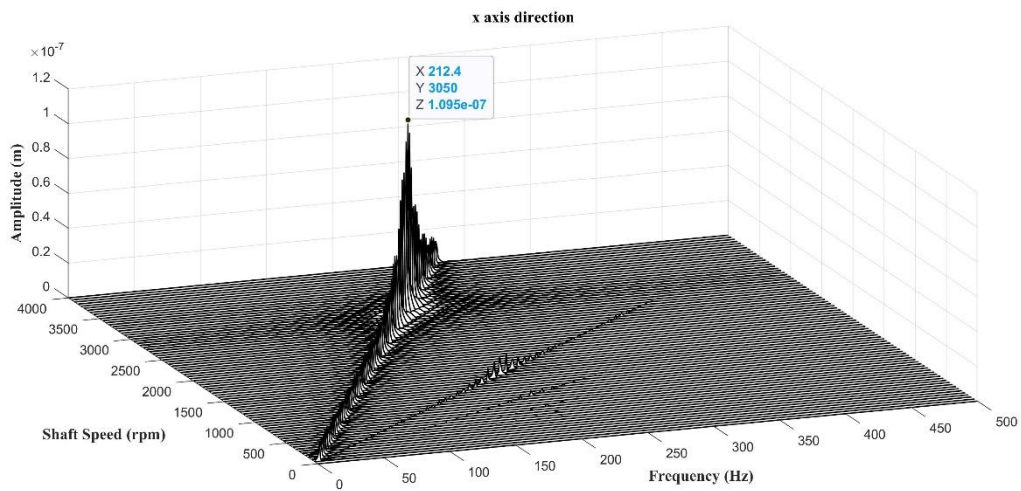


Figure 6. 6203 bearing elastic region shaft vibrations in the x-axis

The behavior of the shaft along the y-axis is similar to the x-axis, but the natural frequency of the shaft along the y-axis is 179.95 Hz. So, the shaft resonance along the y-axis occurs at 2500 rpm, as seen in Fig. 7. It should be noted that the superharmonics of the BPF are also visible in Fig. 6 and Fig. 7. However, their amplitudes, when coinciding with the natural frequencies, are lower than the BPF's.

The natural frequency along the x-axis (212.40 Hz) is higher than the natural frequency along the y-axis (179.95 Hz). The system is modeled as gravity along the x-axis. Due to the nonlinear contact between the ball and the races, the loading along x-axis and y-axis are different. The more loaded contact along the x-axis causes a larger contact area, so the more stiffness along this axis leads to a higher natural frequency.

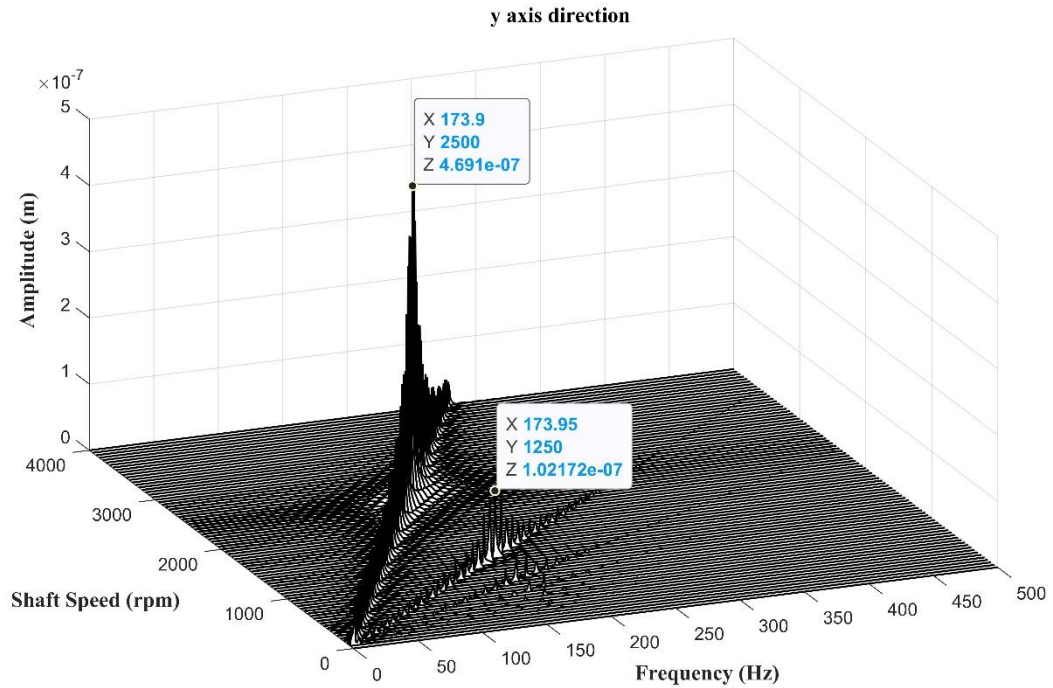


Figure 7. 6203 bearing elastic region shaft vibrations in the y-axis

5. CONCLUSION

Using the indentation contact model, a mathematical model was created to determine the dynamic characteristics of the 6203 polymer hybrid bearing. Since the system is modeled with 2 degrees of freedom, the shaft-bearing system has two natural frequencies along each axis. Gravitational force affects the x-axis, so the natural frequency along this axis is higher than the other axis due to the nonlinear contact between the ball and the races. As can be seen from the waterfall diagrams, resonance occurs when the Ball Pass Frequency (BPF) coincides with one of the system's natural frequencies. Since the resonance zone has a destructive effect, these kinds of systems should not be operated at this shaft speed, or the system's design must be altered to avoid these working conditions.

ACKNOWLEDGMENTS

Gazi University Scientific Research Projects Unit funded the presented study with Grant No. **06/2018-08**.

REFERENCES

1. Ghaednia, H., Pope, S. A., Jackson, R. L., and Marghitu, D. B. A comprehensive study of the elasto-plastic contact of a sphere and a flat. *Tribology International*, 93, 78-90, 2016.
2. Kogut, L., and Etsion, I. Elastic-plastic contact analysis of a sphere and a rigid flat. *Journal of Applied Mechanics*, 69(5), 657-662, 2002.
3. Jackson, R. L., and Green, I. A finite element study of elasto-plastic hemispherical contact against a rigid flat. *Transactions of the ASME-F-Journal of Tribology*, 127(2), 343-354, 2005.
4. Jackson, R. L., and Green, I. A finite element study of elasto-plastic hemispherical contact. *International Joint Tribology Conference*. 37068, 65-72, 2003.
5. Brake, M. R. An analytical elastic-perfectly plastic contact model. *International Journal of Solids and Structures*, 49(22), 3129-3141, 2012.
6. Jamari, J., and Schipper, D. J. Anelastic-plastic contact model of ellipsoid bodies. *Tribology letters*, 21(3), 262-271, 2006.

7. Zhao, Y., Maietta, D. M., and Chang, L. An asperity microcontact model incorporating the transition from elastic deformation to fully plastic flow. *ASME JOURNAL OF TRIBOLOGY*,122(1), 86-93, 2000.
8. Li, L. Y., Wu, C. Y., and Thornton, C. A theoretical model for the contact of elastoplastic bodies. *Proceedings of the Institution of Mechanical Engineers, Part C: Journal of Mechanical Engineering Science*, 216(4), 421-431, 2001.
9. Sharma, A., and Jackson, R. L. A finite element study of an elasto-plastic disk or cylindrical contact against a rigid flat in plane stress with bilinear hardening. *Tribology Letters*, 65(3), 1-12, 2017.
10. Yau, L. C., Zamri, W. F. H. W., Mohamed, I. F., Kamal, A., and Ariffin, M. F. M. D. An Elasto-Plastic Ball Bearing Contact with Bilinear Hardening. *International Journal of Innovative Technology and Exploring Engineering*, 9(4), 2020.
11. Yau, L. C., Zamri, W. F. H. W., Din, M. F. M., Fadhlina, I., and Mohamed, A. A. Elastic and Elasto-Plastic Contact Behavior on Ball Bearing. *International Journal of Innovative Technology and Exploring Engineering*, 8(6), 2020.
12. Song, Z., and Komvopoulos, K. Elastic-plastic spherical indentation: deformation regimes, evolution of plasticity, and hardening effect. *Mechanics of Materials*, 61, 91-100, 2013.
13. Ogar, P., Ugryumova, E., Gorokhov, D., and Zhuk, A. Influence of the of hardenable material on elastoplastic flattening of spherical asperities. *Materials Today: Proceedings*, 38, 1638-1643, 2021,
14. Deng, Q., Yin, X., and Abdel Wahab, M. A Comparative Study on Indentation and Flattening Contacts. *Fracture, Fatigue and Wear*, 67-79, Springer, Singapore, 2020.
15. Ogar, P., Gorokhov, D., and Ugryumova, E. Indentation and flattening of rough surfaces spherical asperities. *International Journal of Engineering and Technology (UAE)*, 7(2.23), 188-191, 2018.
16. Jackson, R. L., and Kogut, L. A comparison of flattening and indentation approaches for contact mechanics modeling of single asperity contacts. *Journal of Tribology*, 128(1), 209-212, 2006.
17. Mesarovic, S. D., and Fleck, N. A. Spherical indentation of elastic-plastic solids. *Proceedings of the Royal Society of London. Series A: Mathematical, Physical and Engineering Sciences*, 455(1987), 2707-2728, 1999.
18. Jackson, R. L., Ghaednia, H., and Pope, S. A solution of rigid-perfectly plastic deep spherical indentation based on slip-line theory. *Tribology Letters*, 58(3), 1-7, 2015.
19. Gustafsson, O. G., and Tallian, T. Study of the vibration characteristics of bearings. *SKF INDUSTRIES INC PHILADELPHIA PA*, 1963.
20. Karaçay T. Açısız Temaslı Rulmanlarla Yataklanmış Şaftların Dinamiği ve Rulman Hatalarının Deneysel Analizi, Doktora Tezi, Gazi Üniversitesi Fen Bilimleri Enstitüsü, Ankara, 2006.
21. Meyer, L. D., Ahlgren, F. F., and Weichbrodt, B. An analytic model for ball bearing vibrations to predict vibration response to distributed defects. *ASME. J. Mech. Des.* 102(2): 205-210, 1980.
22. Patil, M. S., Mathew, J., Rajendrakumar, P. K., and Desai, S. A theoretical model to predict the effect of localized defect on vibrations associated with ball bearings. *International Journal of Mechanical Sciences*, 52.9, 1193-1201, 2010.
23. Mufazzal, S., Muzakkir, S. M., and Khanam, S. Theoretical and experimental analyses of vibration impulses and their influence on accurate diagnosis of ball bearing with localized outer race defect. *Journal of Sound and Vibration*, 513, 116407, 2021.
24. Yu, G., Su, M., Xia, W., Wu, R., and Wang, Q. Vibration characteristics of deep groove ball bearing based on 4-DOF mathematical model. *Procedia Engineering*, 174, 808-814, 2017.
25. Tandon, N., and Choudhury, A. An analytical model for the prediction of the vibration response of rolling element bearings due to a localized defect. *Journal of sound and vibration*, 205(3), 275-292, 1997.
26. Aliustaoğlu, C., Ocak, H. ve Ertunç, H. M. Rulman Titreşim analizi ile bölgesel hataların incelenmesi. *Otomatik Kontrol Ulusal Toplantısı'07 Bildiriler Kitabı*, 451- 456, 2007.
27. Harris, T.A., *Rolling Bearing Analysis* 4th edition, Jon Wiley&Sons, New York, 2001.

APPENDİX - Ball elasticity subroutine

